New structural aspects of Elements appearing under hydrostatic pressure

*K. Takemura**

National Institute for Materials Science (NIMS), Tsukuba, Ibaraki 305-0044 Japan

**E-mail: takemura.kenichi@nims.go.jp*

Introduction

Importance of hydrostaticity in high-pressure research has well been recognized in recent years. Figure 1 illustrates a sample pressurized in a diamond-anvil cell (DAC). If the pressure-transmitting medium is a hard solid, the stress condition in the sample chamber becomes nonhydrostatic, giving rise to a number of problems. Firstly, pressure (or better to say, stress) is anisotropic and spatially inhomogeneous. Pressure on a ruby sensor can be different from that on the sample, if it is located far from the sample. The sample itself suffers from a large pressure gradient, and hence we cannot define the pressure with high precision. Secondly, if the sample is anisotropically compressed, the crystal lattice is distorted. The distorted lattice, if studied by x-ray diffraction, gives lattice parameters different from those under isotropic compression (Singh *et al*. 1998). This is a big problem, for example, for the determination of the equation of state. Phase transition pressures are affected by stress conditions (von Bargen and Boehler 1990), and even the phase stability may become different. More importantly, however, physical properties, such as electrical, magnetic, and optical ones, are likely to be different for such a distorted lattice. Hydrostatic conditions are therefore essential for the study of intrinsic properties of a sample subjected to high pressure.

For diffraction studies with synchrotron sources, hydrostatic conditions are important to get higher angular resolution and reliable diffraction intensity without preferred orientation. Furthermore, hydrostaticity reduces pressure gradients in the sample chamber, thereby minimizing phase mixture near the transition pressure. This unique feature often leads us to identify new phases, which are stable in a small pressure interval and hidden under nonhydrostatic conditions. A good example is the recent discovery of the incommensurate phase of iodine near the molecular dissociation (Takemura *et al*. 2003), where hydrostaticity played a crucial role.

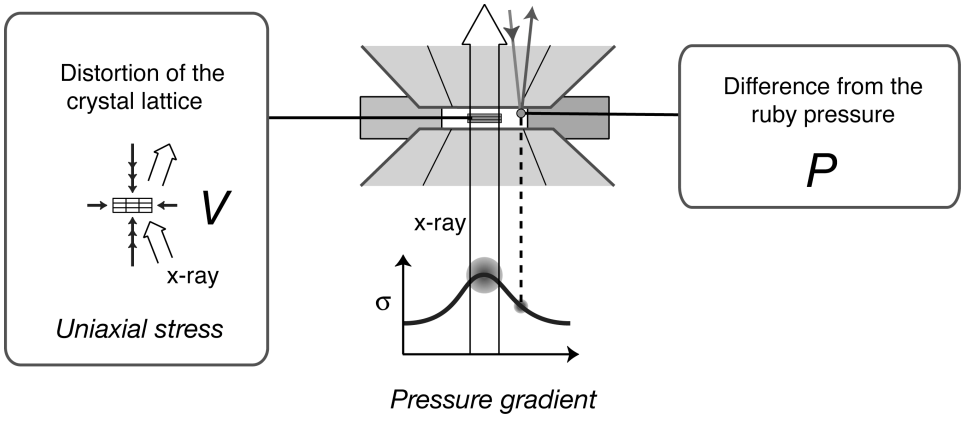

Fig. 1. Schematic view of a sample pressurized in a DAC under nonhydrostatic conditions. Both pressure *P* and volume *V* become highly uncertain under nonhydrostatic compression.

In this talk, I will describe some technical features of hydrostatic experiments with the DAC's, followed by detailed description of the incommensurate phase of iodine. Other examples will also be presented for the structural studies of elemental metals under hydrostatic conditions.

Helium-pressure medium

Helium solidifies at about 12 GPa at room temperature (Besson and Pinceaux 1979). The stress environment given by the He-pressure medium is therefore not purely hydrostatic but quasi-hydrostatic above that pressure. Solid He is, however, very soft to bear negligible shear stress. The pressure gradient in a gasket hole filled with He was determined to be less than 0.4% at 60 GPa by the ruby fluorescence method (Bell and Mao 1981). The good hydrostaticity of He was also confirmed by the powder x-ray diffraction method to at least 50 GPa (Takemura 2001a).

Helium can be loaded to a DAC either as liquid at low temperature (Eremets1996),or high-pressure gas at room temperature (Besson and Pinceaux 1979; Mills *et al*. 1980; Takemura *et al*. 2001b). Since He is very compressible, the gasket hole shrinks to about 70% of the initial size after loading He. The sample size should be small enough not to be compressed directly by the anvils. Pressures can be determined on the basis of the hydrostatic ruby pressure scale (Zha*et al*. 2000).

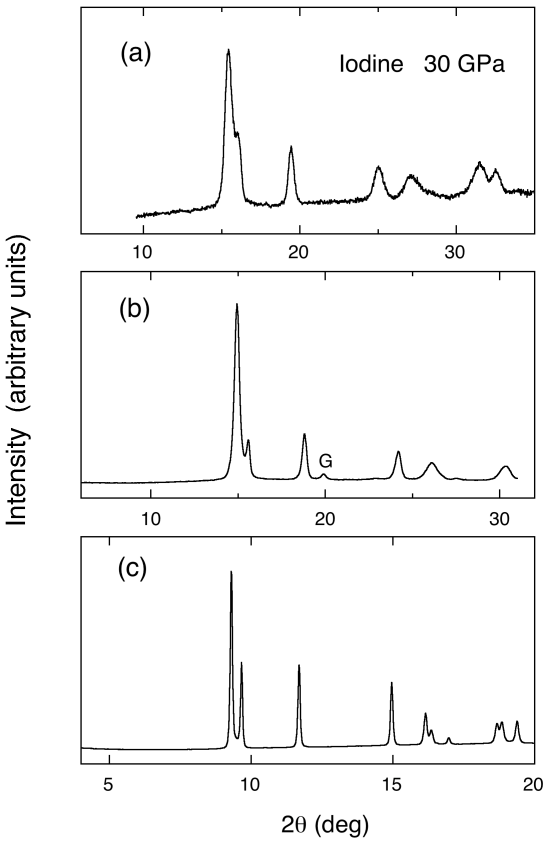

Fig. 2. Powder x-ray diffraction patterns of the high-pressure phase II of iodine at 30 GPa. Experimental conditions (pressure medium, x-ray source, x-ray wavelength, detector) are: (a) no pressure medium, X-ray tube, 0.7107 Å, position-sensitive detector; (b) no pressure medium, synchrotron radiation, 0.6888 Å, imaging plate; (c) He-pressure medium, synchrotron radiation, 0.4264 Å, imaging plate. No background is subtracted in each pattern. G in (b) denotes the diffraction peak by the gasket.

Iodine

Figure 2 compares the powder x-ray diffraction patterns of the high-pressure phase II of iodine taken under different experimental conditions. The pattern (a) was taken with no pressure medium, an x-ray tube, and a position-sensitive detector (Takemura *et al*. 1980). The pattern (b) was taken with no pressure medium, synchrotron radiation (Photon Factory, BL-6B), and an imaging plate (Fujihisa 1990). One notices the improved statistics, which is due to the high brilliance of the synchrotron source and the low background level of the imaging plate. The peak resolution is, however, comparable in both patterns. The pattern (c) was taken with a He-pressure medium, synchrotron radiation (Photon Factory, BL-13A), and an imaging plate (Takemura *et al*. 2003). Although the diffraction system is practically the same for the patterns (b) and (c), the peak resolution is dramatically improved for the latter. This is exactly the effect of the He-pressure medium, which offers good quasi-hydrostatic conditions. In other words, the state-of-art high-pressure diffraction system based on synchrotron sources is best utilized when combined with hydrostaticity.

With the use of a He-pressure medium, we have found a new high-pressure phase of iodine, which exists between 24 and 28 GPa (Takemura *et al*. 2003). The new phase (phase

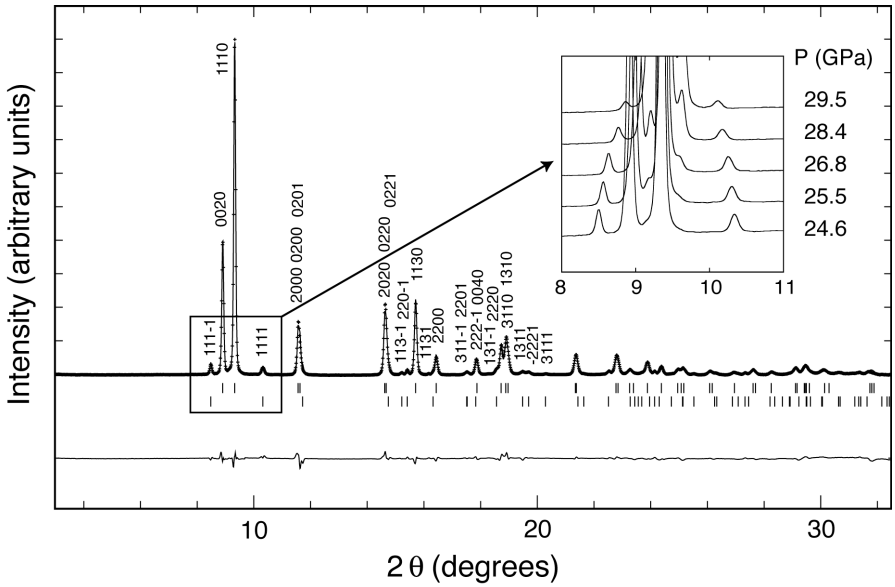

Fig. 3. Powder x-ray diffraction pattern of phase V of iodine at 24.6 GPa taken with a He-pressure medium (figure reproduced from Takemura *et al*. 2004a). The x-ray wavelength was 0.4264 Å. The *hklm* indices are given for reflections at low scattering angles. The upper tick marks below the observed pattern indicate the reflections for the basic face-centered orthorhombic cell, and the lower marks for the satellite reflections. The bottom line shows the residual intensity after refinement. The inset shows the change of the diffraction patterns with pressure.

V) usually coexists with the low-pressure molecular phase (phase I) or the high-pressure monatomic phase (phase II). Only in a small pressure interval of 24-25 GPa, we could obtain the pure diffraction pattern of phase V. In the early investigations (Takemura *et al*. 1980), the diffraction patterns in this pressure range were always a mixture of phase I, II and V, since no pressure medium was used.

Figure 3 shows the diffraction pattern of phase V at 24.6 GPa together with the result of structure refinement. As shown in the inset, an interesting feature of this phase is the shift of some diffraction peaks to lower scattering angles with pressure. This strongly suggests that the peaks are satellite reflections, which approach the main reflections with the change of the modulation wave number. We have successfully indexed the major reflections (upper tick marks in Fig. 3) with a face-centered orthorhombic lattice, and other weak reflections (lower tick marks) as satellite reflections produced by structural modulation.

Figure 4 shows the structural model for phase V. The structure is incommensurately modulated, in which the modulation wave propagates along the *a*-axis of the basic cell. We assume that the modulation wave is simple sinusoidal one (Takemura *et al*. 2003, 2004a). The atoms are displaced in the direction of the *b*-axis as shown below the structure. The modulation wavelength *1/k* is close but not equal to four. The crystal structure can be represented as *Fmm2*(α00)0s0 in the four-dimensional space group. As a result of the structural modulation, the interatomic distances become different place by place, giving rise to a continuous distribution of the nearest interatomic distance. Figure 5 compares the crystal structure of phases I, V and II of iodine. The change with pressure of the interatomic distances is summarized in Fig. 6. Phase I has a well-defined molecular bond (distance 1-2) at 2.7-2.8 Å, while no such a molecular bond exists in phase II. Instead, the atoms in phase II are nearly uniformly distributed in the former molecular plane (Fig. 5), which characterizes it as a monatomic phase. The nearest interatomic distances of phase V just fall in between those for phases I and II. We therefore consider phase V to be the transient state between the molecular and monatomic phases (Takemura *et al*. 2003, 2004a).

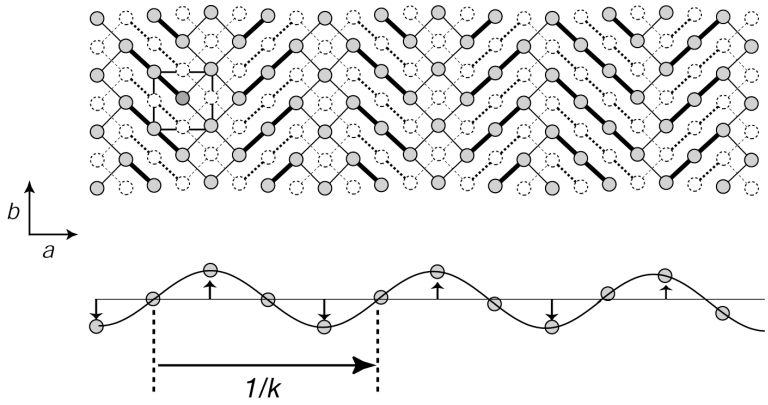

Fig. 4. Structural model for phase V of iodine at 24.6 GPa (figure reproduced from Takemura *et al.* 2004a). The square in the upper figure shows the basic face-centered orthorhombic cell. The thick bonds indicate the interatomic distances shorter than 2.92 Å, and the thin bonds those at 2.92-3.05 Å. The modulation wave is schematically shown below, in which the modulation amplitude is exaggerated for clarity.

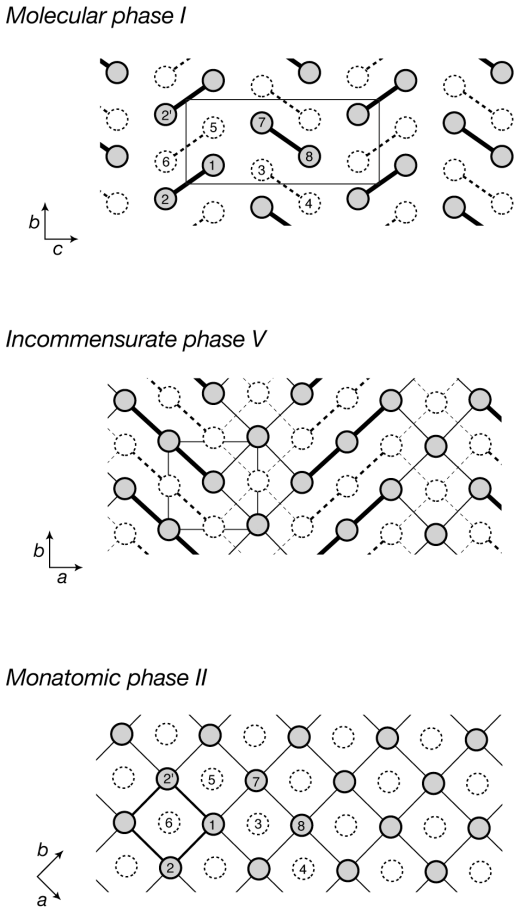

Fig. 5. Crystal structure of phase I (19.1 GPa), V (24.6 GPa), and II (30.4 GPa) of iodine (figure reproduced from Takemura *et al.* 2004a). The atoms drawn by broken lines lie on the plane half-way below the respective plane.

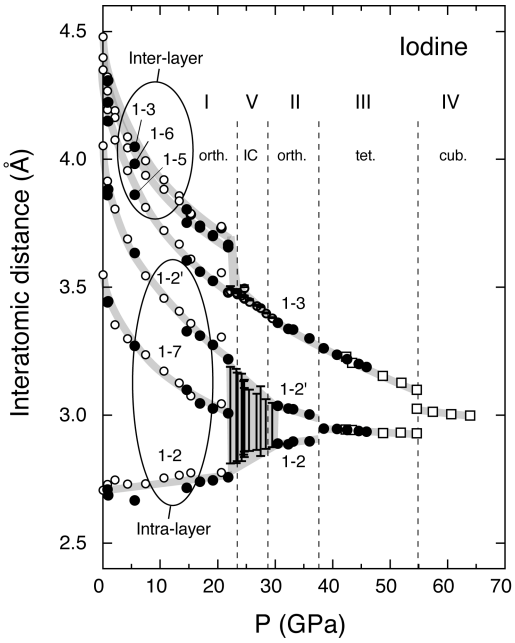

Fig. 6. Change in the interatomic distances of iodine with pressure (figure reproduced from Takemura *et al.* 2004a). The numbers like 1-2 mean the distances between the atoms labeled in Fig. 5. The interatomic distances for phase V are not discrete but have distribution shown by the vertical bars.

Zinc and osmium

Zinc has been calculated to undergo a pressure-induced electronic topological transition, and may reveal it as a lattice anomaly (Fast *et al*. 1997). Early diffraction study actually seemed to observe it (Takemura 1995), but later experiments with the He-pressure medium showed no evidence for the anomaly as seen in Fig. 7 (Takemura 1999). The anomaly reported in the former experiment was most likely caused by the discontinuous change in the stress conditions, when the methanol-ethanol-water pressure medium solidified at high pressures. Although many calculations on Zn suggest small but definite lattice anomalies at the electronic topological transitions (See, for example, Novikov *et al*. 1997; Li and Tse 2000; Kechin 2001; Qiu and Marcus 2003), no clear experimental evidence exists for the moment. Further experimental efforts are necessary to resolve the controversy of Zn under pressure, but any high-pressure experiments should pay special attention to the hydrostaticity. Zinc, as a highly anisotropic metal, is extremely sensitive to nonhydrostatic stress.

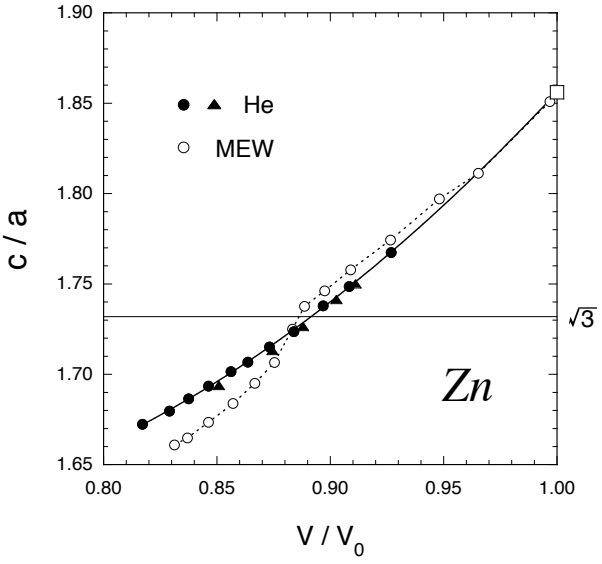

Fig. 7. The *c/a* axial ratio of Zn as a function of relative volume V/V_0 (figure reproduced from Takemura 1999). Open circles show the data in the early measurement (Takemura 1995) with the methanol-ethanol-water (MEW) pressure medium. Closed circles show the data with the He-pressure medium (Takemura 1999).

The bulk modulus of osmium has been the focus of recent high-pressure studies. The first report (Cynn *et al*. 2002) showed that the bulk modulus of Os exceeds that of diamond, the hardest known material. Later experimental studies by other groups, however, did not confirm the result, showing that the bulk modulus of Os is close to but slightly smaller than that of diamond (Takemura 2004b; Occelli *et al*. 2004). An important difference between the first report and the other is the pressure medium: Ar was used in the former work, while He was used in the latter works. Although Ar is a good (hydrostatic) pressure medium at low pressures, it gradually develops shear stress at pressures higher than 9 GPa (Bell and Mao 1981). Diffraction data taken with the Ar-pressure medium, specifically above 20 GPa, should be carefully evaluated to check the effects of nonhydrostaticity. See this proceedings for more details (Takemura *et al*. 2005).

Discussion

The examples given above demonstrate the power of the He-pressure medium in the powder x-ray diffraction experiments. Helium is clearly the best pressure medium in the pressure range up to about 50 GPa. At ultrahigh pressures, however, even helium may become hard and give shear stress to the sample. It is predicted that the closed-shell electron configuration of rare gas solids makes them rapidly hard under high compression (Brazhkin and Lyapin 2002). Brazhkin and Lyapin propose that ionic solids or metals can be better pressure media rather than rare gas solids in the megabar pressure range. Of course the choice of pressure media depends on other factors such as chemical inertness, scattering factor and transparency. Because He fulfills the most requirements as a pressure medium, the ultimate limit of its hydrostaticity at ultrahigh pressures should be further investigated.

Another point to be mentioned is the difficulty to realize the ideal sample configuration at ultrahigh pressures. Since the metal gasket in general becomes very thin (~few micron) at ultrahigh pressures, it is quite difficult to keep the sample and ruby apart from the anvil face.

Hydrostatic experiments at ultrahigh pressures are therefore challenging and need technical developments including gasket material. It is well known that He often breaks diamond anvils at high pressures. The exact mechanism is not well understood, but the large discontinuity in stress at the edge of the gasket hole may cause cracks in the diamonds. Some techniques should be developed to avoid the failure of diamond anvils for the wider use of the He-pressure medium in the high-pressure community.

Finally, it should be mentioned that hydrostatic or quasi-hydrostatic conditions are also achieved by annealing samples in the DAC at high pressures. External or laser-heating can be used for this purpose as demonstrated, for example, by Leger *et al.* (1995).

Conclusion

The use of the He-pressure medium dramatically improves the quality of high-pressure data specifically in the pressure range above 10 GPa, where the conventional alcohol pressure media solidify and develop large shear stress. New structural aspects emerge as demonstrated for iodine, or accidental anomalies may disappear as shown for zinc. Many previous experiments are worth investigating again with He in order to check the validity of old "anomalies". Regarding to the structural studies at high pressures, one has better chance to solve the complex structures of high-pressure phases, as the He-pressure medium gives excellent diffraction patterns with higher resolution, accurate peak positions, and reliable diffraction intensities.

Acknowledgement

The author thanks K. Sato, H. Fujihisa, M. Onoda, A. Yamamoto, S. Nakano, Y. Ohishi, and T. Kikegawa for their collaboration. Powder x-ray diffraction experiments at the Photon Factory have been done under Proposal Nos. 2001G225 and 2003G200.

References

Bell P. M., Mao H. K., 1981. Degrees of hydrostaticity in He, Ne, and Ar pressure-transmitting media. *Carnegie Inst. Washington Publ.* **80**, 404-406.

Besson J. M., Pinceaux J. P., 1979. Melting of helium at room temperature and high pressure. *Science* **206**, 1073-1075.

Brazhkin V. V., Lyapin A. G., 2002. The inversion of relative shear rigidity in different material classes at megabar pressures. *J. Phys.: Condens. Matter* **14**, 10861-10867.

Cynn H., Klepeis J. E., Yoo C.-S., Young D. A., 2002. Osmium has the lowest experimentally determined compressibility. *Phys. Rev. Lett.* ***88,*** *1*35701.

Eremets M. I., 1996. *High Pressure Experimental Methods.* Oxford: Oxford Univ. Press.

Fast L., Ahuja R., Nordström L., Wills J. M., Johansson, B., Eriksson O., 1997. Anomaly in *c/a* ratio of Zn under pressure. *Phys. Rev. Lett.* **79**, 2301-2303.

Fujihisa H., 1990. (unpublished).

Kechin V. V., 2001. Electronic topological transitions in Zn under compression. *Phys. Rev. B* **63**, 045119.

Leger J. M., Haines J., Atouf A., Schulte O., Hull S., 1995. High-pressure x-ray- and neutron-diffraction studies of BaF_2: An example of a coordination number of 11 in AX_2 compounds. *Phys. Rev. B* **52**, 13247-13256.

Li Z., Tse J. S., 2000. Phonon anomaly in high-pressure Zn. *Phys. Rev. Lett.* **85**, 5130-5133.

Mills R. L., Liebenberg D. H., Bronson J. C., Schmidt L. C., 1980. Procedure for loading diamond cells with high-pressure gas. *Rev. Sci. Instrum*. **51**, 891-895.

Novikov D. L., Freeman A. J., Christensen N. E., Svane A., Rodriguez C. O., 1997. LDA simulation of pressure-induced anomalies in *c/a* and electric-field gradients for Zn and Cd. *Phys. Rev. B* **56**, 7206-7214.

Occelli F., Loubeyre P., LeToullec R., 2003. Properties of diamond under hydrostatic pressures up to 140 GPa. *Nature Materials* **2**, 151-154.

Occelli F., Farber D. L., Badro J., Aracne C. M., Teter D. M., Hanfland M., Canny B., Couzinet B., 2004. Experimental evidence for a high-pressure isostructural phase transition in osmium. *Phys. Rev. Lett.* **93**, 095502.

Qiu S. L., Marcus P. M., 2003. First-principles derivation of structural anomalies in hcp Zn and hcp Fe under pressure. *J. Phys.: Condens. Matter* **15**, L755-L761.

Singh A. K., Balasingh C., Mao Ho-kwang, Hemley R. J., Shu J., 1998. Analysis of lattice strains measured under nonhydrostatic pressure. *J. Appl. Phys.* **83**, 7567-7575.

Takemura K., Minomura S., Shimomura O., Fujii Y., 1980. Observation of molecular dissociation of iodine at high pressure by x-ray diffraction. *Phys. Rev. Lett.* **45**, 1881-1884.

Takemura K., 1995. Zn under pressure: a singularity in the hcp structure at *c/a* =√3. *Phys. Rev. Lett.* **75**, 1807-1810.

Takemura K., 1999. Absence of the *c/a* anomaly in Zn under high pressure with a helium-pressure medium. *Phys. Rev. B* **60**, 6171-6174.

Takemura K., 2001a. Evaluation of the hydrostaticity of a helium-pressure medium with powder x-ray diffraction techniques. *J. Appl. Phys.* **89**, 662-668.

Takemura K., Sahu P. Ch., Kunii Y., Toma Y., 2001b. Versatile gas-loading system for diamond-anvil cells. *Rev. Sci. Instrum.* **72**, 3873-3876.

Takemura K., Sato K., Fujihisa H., Onoda M., 2003. Modulated structure of solid iodine during its molecular dissociation under high pressure. *Nature (London)* **423**, 971-974.

Takemura K., Sato K., Fujihisa H., Onoda M., 2004a. Structural phase transitions in iodine under high pressure. *Z. Kristallogr.* **219**, 749-754.

Takemura K., 2004b. Bulk modulus of osmium: High-pressure powder x-ray diffraction experiments under quasihydrostatic conditions. *Phys. Rev. B* **70**, 012101.

Takemura K., Arai M., Kobayashi K., Sasaki T., 2005. Bulk modulus of osmium by experiments and first-principles calculations. (in this proceedings).

von Bargen N., Boehler R., 1990. Effect of non-hydrostaticity on the α-ε transition of iron. *High Press. Res.* **6**, 133-140.

Zha Chang-Sheng, Mao Ho-kwang, Hemley R. J., 2000. Elasticity of MgO and a primary pressure scale to 55 GPa. *Proc. Natl. Acad. Sci.* **97**,13494-13499.